AmerGen Energy Company, LLC
Three Mile Island Unit 1
Route 441 South, P.O. Box 480
Middletown, PA 17057

Telephone: 717-944-7621

AmerGen SM

An Exelon/British Energy Company

January 18, 2002
5928-01-20338

U.S. Nuclear Regulatory Commission
ATTN: Document Control Desk
Washington, DC 20555-0001

SUBJECT: Response to NRC Staff Follow-Up Questions 5 through 15 from November 9, 2001 Meeting Regarding a TMI Unit 1 Steam Generator Severed Tube

THREE MILE ISLAND, UNIT 1 (TMI UNIT 1)
OPERATING LICENSE NO. DPR-50
NRC DOCKET NO. 50-289

References:
1. NRC Letter, "Summary of November 9, 2001, Meeting with AmerGen Regarding TMI-1 Steam Generator Severed Tube Root Cause (TAC MB3305)," dated November 21, 2001.
2. AmerGen Letter to NRC, "Response to NRC Staff Follow-Up Questions 1 through 4 From November 9, 2001 Meeting Regarding a TMI Unit 1 Steam Generator Severed Tube," dated November 26, 2001.
3. AmerGen Letter to NRC, "Licensee Event Report (LER) No. 2001-003-00, 'Degraded OTSG Tube,'" dated December 14, 2001.

On November 9, 2001 AmerGen made a presentation to the NRC regarding a plugged tube in the "B" Once-Through Steam Generator (OTSG) that was discovered during the T1R14 refueling outage eddy current examinations to have severed and caused wear damage to adjacent tubes. This was reported to the NRC in Licensee Event Report (LER) 2001-003-00 (Reference 3).

Enclosure 4 to the NRC's meeting summary (Reference 1) was a list of 15 questions. In accordance with the meeting summary, responses to questions 1 through 4 were provided on November 26, 2001 (Reference 2) and responses to questions 5 through 15 are enclosed as Attachment 1 to this letter.

The responses in Attachment 1 supersede any preliminary information provided to the NRC Special Inspection team during the T1R14 outage where any differences may exist.

A001

Attachment 1 contains information proprietary to Framatome ANP (FRA-ANP). An affidavit from FRA-ANP is included which sets forth the basis on which the information may be withheld from public disclosure by the NRC pursuant to 10 FR 2.790. Attachment 2 provides a non-proprietary version of this response.

Very truly yours,

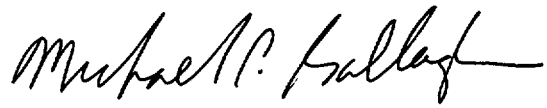

Michael P. Gallagher
Director – Licensing and Regulatory Affairs
Mid-Atlantic Regional Operating Group

Attachments: 1) Proprietary Version of Response
2) Non-Proprietary Version of Response
3) Framatome Paper on Adaptation of PORTHOS to OTSGs

cc: H. J. Miller, USNRC, Regional Administrator, Region I
T. G. Colburn, USNRC, Senior Project Manager, TMI Unit 1
J. D. Orr, USNRC, Senior Resident Inspector, TMI Unit 1
File No. 01076

Attachment 1
(Proprietary Version)

Response to NRC Follow-Up Questions 5 Through 15 from November 9, 2001 Meeting Regarding the TMI Unit 1 Steam Generator Severed Tube Root Cause

AFFIDAVIT

COMMONWEALTH OF VIRGINIA)
) ss.
CITY OF LYNCHBURG)

1. My name is James F. Mallay. I am Director, Regulatory Affairs, for Framatome ANP ("FRA-ANP"), and as such I am authorized to execute this Affidavit.

2. I am familiar with the criteria applied by FRA-ANP to determine whether certain FRA-ANP information is proprietary. I am familiar with the policies established by FRA-ANP to ensure the proper application of these criteria.

3. I am familiar with the FRA-ANP information contained in the attachment to a letter from Framatome ANP to AmerGen Energy Company of January 15, 2002, FANP-02-100. This attachment is referred to herein as "Document." Information contained in this Document has been classified by FRA-ANP as proprietary in accordance with the policies established by FRA-ANP for the control and protection of proprietary and confidential information.

4. This Document contains information of a proprietary and confidential nature and is of the type customarily held in confidence by FRA-ANP and not made available to the public. Based on my experience, I am aware that other companies regard information of the kind contained in this Document as proprietary and confidential.

5. This Document has been made available to the U.S. Nuclear Regulatory Commission in confidence with the request that the information contained in the Document be withheld from public disclosure.

6. The following criteria are customarily applied by FRA-ANP to determine whether information should be classified as proprietary:

(a) The information reveals details of FRA-ANP's research and development plans and programs or their results.

(b) Use of the information by a competitor would permit the competitor to significantly reduce its expenditures, in time or resources, to design, produce, or market a similar product or service.

(c) The information includes test data or analytical techniques concerning a process, methodology, or component, the application of which results in a competitive advantage for FRA-ANP.

(d) The information reveals certain distinguishing aspects of a process, methodology, or component, the exclusive use of which provides a competitive advantage for FRA-ANP in product optimization or marketability.

(e) The information is vital to a competitive advantage held by FRA-ANP, would be helpful to competitors to FRA-ANP, and would likely cause substantial harm to the competitive position of FRA-ANP.

7. In accordance with FRA-ANP's policies governing the protection and control of information, proprietary information contained in this Document has been made available, on a limited basis, to others outside FRA-ANP only as required and under suitable agreement providing for nondisclosure and limited use of the information.

8. FRA-ANP policy requires that proprietary information be kept in a secured file or area and distributed on a need-to-know basis.

9. The foregoing statements are true and correct to the best of my knowledge, information, and belief.

SUBSCRIBED before me this 15th day of January, 2002.

Ella F. Carr-Payne
NOTARY PUBLIC, STATE OF VIRGINIA
MY COMMISSION EXPIRES: 08/31/05

ELLA F. CARR-PAYNE
Notary Public
Commonwealth of Virginia
My Commission Exps. Aug. 31, 2005

Attachment 2
(Non-Proprietary Version)

Response to NRC Follow-Up Questions 5 Through 15 from November 9, 2001 Meeting Regarding the TMI Unit 1 Steam Generator Severed Tube Root Cause

This attachment contains the non-proprietary version of the responses to NRC questions provided by Framatome ANP (FRA-ANP). In order to qualify as a non-proprietary document, certain blocks of proprietary information have been withheld. The criteria used for withholding information are provided below.

(a) The information reveals details of FRA-ANP's research and development plans and programs or their results.

(b) Use of the information by a competitor would permit the competitor to significantly reduce its expenditures, in time or resources, to design, produce, or market a similar product or service.

(c) The information includes test data or analytical techniques concerning a process, methodology, or component, the application of which results in a competitive advantage to FRA-ANP.

(d) The information reveals certain distinguishing aspects of a process, methodology, or component, the exclusive use of which provides a competitive advantage for FRA-ANP in product optimization or marketability.

(e) The information is vital to a competitive advantage held by FRA-ANP, would be helpful to competitors to FRA-ANP, and would likely cause substantial harm to the competitive position of FRA-ANP.

In this non-proprietary version, proprietary information has been deleted and replaced by brackets containing the letter designators for the above criteria for which the information is being withheld.

Response to NRC Follow-Up Questions 5 Through 15 from November 9, 2001 Meeting Regarding the TMI Unit 1 Steam Generator Severed Tube Root Cause

5. Has TMI-1 experienced any denting at the tube sheets or tube support plates? If so, summarize the extent and magnitude.

Response:

TMI Unit 1 has had a history of dents at the tubesheet secondary faces and tube support plates (TSPs). During the T1R14 Outage, AmerGen performed Motorized Rotating Pancake Coil (MRPC) examinations of all Upper Tubesheet (UTS) secondary face dents, 33% of the dents above the Lower Tubesheet (LTS), approximately 33% of the dents inside the LTS kidney examination region, and all LTS dents outside the kidney exam region that were >16 volts. No PWSCC or ODSCC indications were identified at these locations.

The tables below list the T1R14 Outage dent indications identified at the UTS and LTS secondary faces and the TSPs. The voltage information in this table is based on 400 kHz bobbin coil differential signals from the four 20% through wall drilled holes set equivalent to 4 volts on the BWOG mother ASME standard and normalizing to all other channels. Dents are recorded when the 400/200 kHz differential mix dent signal measures $\geq$ 2.5 volts.

Outage 1R14 OTSG-A TSP and Tubesheet Secondary Face Dent Summary

Location	Quantity of Dents	Average Voltage	Maximum Voltage
UTS Secondary Face	124	3.1	11.3
LTS Secondary Face	287	9.9	91.3
TSP Locations	4	3.2	4.1

Outage 1R14 OTSG-B TSP and Tubesheet Secondary Face Dent Summary

Location	Quantity of Dents	Average Voltage	Maximum Voltage
UTS Secondary Face	114	3.0	14.9
LTS Secondary Face	1046	10.8	73.0
TSP Locations	3	3.7	4.5

6. Describe the adaptation of PORTHOS to once-through steam generators (OTSGs). Assess the uncertainty of the velocity predictions from PORTHOS. Discuss the ability of PORTHOS to predict local cross flow velocities for the actual tube array geometry. For example, does PORTHOS model the differences in flow resistance for radial flow parallel to the bundle Y-axis, versus that for radial flow 30, 60, and 90 degrees from the Y-axis?

Response:

Adaptation of PORTHOS to OTSGs

Framatome ANP (FRA-ANP) uses a modified version of EPRI's "PORTHOS" computer code to predict detailed thermal-hydraulic performance of the OTSG. "PORTHOS" is a three-dimensional computational fluid dynamics computer code that models the tube bundle between the lower and upper tubesheet secondary faces. This modified version of "PORTHOS" has been adapted for OTSGs and its accuracy has been documented by FRA-ANP. The OTSG thermal hydraulic model includes the aspirator port, tube support plates, peripheral gap between the tube support plates and the shroud, open tube inspection lane, and steam annulus. The current version does not include the feedwater downcomer, but does include the effects of steam-condensation heating of the feedwater.

The EPRI version of PORTHOS lacks a turbulence model, which limits the ability of the code to represent effects of fluid entrainment by the flow of streams jetting through the OTSG downcomer orifice. Accurate representation of these OTSG effects is required to accurately predict the formation of any recirculation eddies.

Modifications to the PORTHOS coding have been made for the purpose of adding capability to model the orifice plate openings, lower downcomer, and baffle ports in the inlet region of the OTSG. PORTHOS models of the Chalk River (See response to Question 9) and Alliance Research Center steam generator (OTSG) model configurations have been made and results compared with test data. PORTHOS results for velocity distributions over the steam generator inlet region at the tube bundle outer radius are reasonable when compared to this test data. A conservative method is used to extrapolate velocity distributions at the outer radius to other radial locations within the lower bundle.

Additional details relating to the adaptation of PORTHOS to OTSGs are given in the paper, "Adaptation of PORTHOS to the Once-Through Steam Generator," which is included as Attachment 3.

Verification of Predicted Velocities

Thermal hydraulic method accuracy has been verified through favorable comparisons with model scale testing and plant data. These comparisons include:

- Two different tests on 19 and 37 Tube Model Boiler tubes defining axial primary, tube, and secondary temperature distributions over the axial length as well as secondary pressure distributions

- Babcock-Atlantique Tube Bundle Cross Flow Velocity Distributions (with and without internal Auxiliary Feedwater Headers)

- Plant Mixed Mean Steam Temperatures for 2568 Mwt nominal, 2772 Mwt nominal, 2568 Mwt with high peripheral plugging, and 2568 Mwt with three-tube wide inspection lane.

Additional details of the comparisons with test data are given in the paper, "Adaptation of PORTHOS to the Once-Through Steam Generator," which is included as Attachment 3.

Reasonable correlations with plant mixed mean steam temperatures have been made. Therefore, the use of PORTHOS to predict the OTSG secondary side conditions in the top span is justified for use as inputs into subsequent structural and flow-induced vibration (FIV) calculations.

Prediction of Cross Flow Velocity for Various Tube Array Geometries

The PORTHOS computer code uses several values to account for the "porosity" of a steam generator tube bundle in its formulation. The volumetric porosity is used in the computation of cell pressures and the directional porosity values are used to compute gap velocities between the tubes. Directional porosity values are input for the axial, radial, and azimuthal directions. Typically, the axial porosity is set equal to the volumetric porosity. The radial (β_r) and azimuthal (β_θ) porosity values are calculated using the tube pitch and tube diameter as follows:

β_r = (Azimuthal Tube Pitch(θ) – Tube Diameter)/Azimuthal Tube Pitch(θ)

β_θ = (Radial Tube Pitch(θ) – Tube Diameter)/Radial Tube Pitch(θ)

Where the azimuthal and radial tube pitch varies with azimuthal position

The Once-Through Steam Generator tubes are spaced on a triangular pitch. Thus, the tube orientation provides what appears to be a staggered alignment in some directions and an in-line alignment in others. Mathematically, referenced from the center of the tube bundle, this would result in the radial porosity being a minimum along the inspection lane, reaching a maximum 30° away from the lane, followed by a maximum at 60°, a minimum at 90°, and so forth. The azimuthal porosity would trend opposite with maximums at 0°, 60°, 120°, etc. and minimums at 30°, 90°, 150°, etc. It could be suggested that this would result in a "Rosette" pattern of azimuthally-varying radial velocities.

FRA-ANP has concluded that this azimuthal variation is not realistic and that the flow velocities do not exhibit this behavior to any significant extent. The hydraulic resistance of the tube bundle does not have a significant azimuthal dependence and

the azimuthal variation in radial velocities is small. Thus, in PORTHOS modeling, the smaller of the two directional porosity values has been input for both the radial and azimuthal porosity. This maximizes the velocities and is therefore conservative.

7. Nominally, what is the mechanism for flow induced vibration (FIV) in areas such as the peripheral zone of the upper span (Region 1) the lane region of the upper span (Region 2) and peripheral zone of the lower most span (Region 3)? Describe the supporting evidence or basis.

Response:

Flow-induced vibration of heat exchanger tube bundles is discussed in the 2000 Edition of ASME Standard and Guide on the Operation of Nuclear Plants, Part 11, Appendix A, and also in Sec III, Appendix N, paragraph N-1300 of the 1998 Edition of the ASME Boiler and Pressure Vessel Code. According to both codes, the three principal mechanisms for flow-induced vibration of heat exchanger tube bundles are: Fluid-elastic instability, turbulence-induced vibration and vortex-induced vibration. The following gives a very brief description of each of these mechanisms. More details can be found in OM11 and Sec III Appendix N.

Fluid-elastic Instability

This refers to the sudden rapid increase in the vibration amplitude of a tube bundle when the cross-flow velocity over it increases beyond a certain value commonly referred to in the literature as the critical velocity. This is the most detrimental FIV mechanism in tube bundles. In practice the vibration amplitudes of a fluid-elastically unstable tube bundle are limited only by adjacent structural boundaries. This mechanism does not exist in isolated tubes. Isolated tubes or tube bundles with large pitch-to-diameter ratios will not become unstable.

Turbulence-induced Vibration

This mechanism exists in isolated tubes as well as in tube bundles and is caused by the fluctuating component of the dynamic pressure in the turbulent flow over the tubes. Turbulence-induced vibration can be caused by either axial flow or cross flow. The latter is commonly referred to in the literature as turbulent buffeting. As stated in ASME Sec III Appendix N, for the same fluid velocity and density, cross flow turbulence induced vibrations are of much larger amplitudes (more than one order of magnitude) than those caused by axial flows. For this reason, axial flow-induced vibration is ignored in the FIV analysis of OTSG tubes.

Vortex-induced Vibration

Vortex-induced vibration is caused by the alternate shedding of vortices from structures subjected to cross flows. As stated in ASME OM11, vortex induced vibration is of much less concern in tube bundles than in isolated tubes.

Potentially, all three flow-induced vibration mechanisms exist in all three regions. However, in the bottom span (Region 3), the shell-side fluid is two-phase. The chaotic nature of two-phase flow, together with the damping inherent in a two-phase mixture, helps to suppress organized vortex shedding and no vortex shedding has ever been observed in two-phase flows. For this reason, vortex-induced vibration is not considered for the bottom span.

The applicability of each of these mechanisms to the various regions of the OTSG and the methodologies to assess their impacts on the integrity of the tubes are further discussed as part of the answers to questions 8 through 13.

8. Describe the analytical models for evaluating the OTSG tube bundle for FIV and their justification or basis. Describe the model boundary conditions and their justification or basis. Describe the applied loadings, including cross flow velocities and axial load and their justification or basis. Describe the other model input parameters (e.g., damping coefficients) and various model coefficients and constants and their justification or basis. Discuss the source and magnitude of model uncertainties.

Response:

FRA-ANP follows closely the methodologies recommended in ASME Sec III Appendix N for estimating the FIV responses due to the three excitation mechanisms described under response to Question 7 above. In the following, the analytical model, boundary conditions and loading that were used to calculate the FIV responses to all three excitation mechanisms are described first, followed by excitation mechanism specific inputs.

Analytical Models and Boundary Conditions Common to all Three FIV Mechanisms

The FIV response to each excitation mechanism is calculated using finite element techniques provided by FRA-ANP computer codes. The structural model includes the full length of the tube, from the upper tubesheet secondary face (UTSF) to the lower tubesheet secondary face (LTSF), with 20 elements to represent each of the top and bottom spans and 10 elements to represent each of the intermediate spans. The tube is assumed to be fixed at the UTSF and the LTSF due to the very small clearances between the tube and tubesheet. This is a conservative assumption, since the tube motion in the small annulus would increase the damping and therefore reduce the vibratory response. The tube is assumed to be pinned at all 15 TSP locations. This allows rotation and axial movement of the tube relative to the TSP, but allows no

horizontal motion. The effective mass of the tube, including the mass of the primary fluid and the added mass due to the secondary fluid, is considered in the modal analysis. The added mass due to the secondary fluid is computed based on an industry-accepted equation that accounts for the effect of the surrounding tubes.

Applied Loading Common to all Three FIV Mechanisms

The cross flow velocities and fluid densities from PORTHOS are used to compute dynamic loading, which are applied to the single tube model. These thermal hydraulic inputs are determined along the length of the OTSG tube and applied to the entire tube structural model to evaluate the FIV response of the tube. The density and velocity distribution along the length of the bottom and top span was divided into twenty divisions to accurately model this input.

The density and velocity distribution in the top and bottom spans vary significantly in the radial direction of the OTSG. Therefore, the thermal hydraulic data computed with PORTHOS was determined at radial increments of approximately three inches. The FIV response of the tube was also determined at each of these radial locations.

Axial tube loads for various transient and steady state conditions have been calculated using a detailed finite element model of the OTSG. Since the OTSG tubes experience a compressive axial load at 100% power steady state conditions, the natural frequencies of the tube are lower in comparison to a tube that is not under compressive loading. The compressive axial load will therefore lower the Fluid-elastic Stability Margin of the tube.

The compressive axial load varies in the radial direction of the OTSG for an un-swollen tube. When the tube swells due to over pressurization, the Poisson's effect creates a tensile axial load in the tube that will eliminate the compressive load and yields a net tensile load in the tube. The swollen tube residual tensile load is estimated to be approximately 1000 lbs. The FIV analysis evaluated tensile loads ranging from 0 to 1000 lbs even though only those with 1000 lbs axial load are reported.

<u>Methodology, Model Inputs and Basis Specific to Fluid-elastic Instability</u>

Following ASME Sec III Appendix N1300 recommendation, Connors' equation was used to estimate the fluid-elastic stability margins (FSM) of in-service, plugged and plugged and swollen tubes. This semi-empirical equation enabled the critical velocity for instability to be calculated based on a single-tube model. The effect of fluid-structure coupling is accounted for by three parameters:

- Fluid-elastic stability constant, commonly referred to as the Connors' constant. This constant is measured experimentally. Based on both data in the open literature and FRA-ANP proprietary data, a Connors' constant of 3.3 is used. This value lower-bounds approximately 90% of all the published data, and is lower than FRA-ANP's measured value based on the OTSG tube array geometry. It is also within the bounds of ASME's recommended values. In general, a lower Connors' constant

gives more conservative results.

- Added mass due to secondary side fluid, discussed previously under the paragraph on analytical models common to all three excitation mechanisms.

- Added damping due to the secondary side fluid. FRA-ANP calculated very small added damping due to the secondary side fluid. This is because of the low kinematic viscosity associated with water or steam at temperatures higher than 500°F. FRA-ANP's experience is supported by a statement in the 2000 Edition of ASME Sec III Appendix N1470 on added damping of nuclear reactor internal components. For this reason, added damping is ignored in FIV analysis of OTSG tubes.

Other inputs for computing the fluid-elastic stability margins include:

- The mode shape eigenvalues from the modal analysis, computed with the finite element model discussed previously under analytical models.

- The linear mass densities of the tube, including the mass of fluid inside the tube and the added masses discussed earlier.

- Damping ratios. This is based on extensive data obtained from tests involving single tubes, selected tubes in an as-built OTSG, and from recent tests on tubes with nominal as-built tube-to-support plate clearance, tightly supported tubes with no tube-to-support plate clearance, and swollen tubes with pressure inside the tube, with pressure released and with air or water inside the tubes. All of FRA-ANP's test data support the conclusion that most of the damping in a normal operating OTSG tube originates from the relative motion between the tube and the support plates, which results in the observed normal operational wear but also is a means of dissipating energy. Since larger vibration amplitudes dissipate more energy, the damping ratios in OTSG tubes are dependent on the vibration amplitudes. By definition, a fluid-elastically unstable tube vibrates with large amplitudes (compared with the diameter of the tube).

  The bottom span of the OTSG is a region of two-phase flow, where the void fraction (fraction of volume of steam to the total volume of water-steam mixture) is between 20 and 80%. Data from tests conducted at EPRI, Chalk River Nuclear Laboratory and in Japan show there is at least an additional 2% of damping on the tubes in this region. This is commonly referred to as two-phase damping.

  Based on all the above-discussed data, the following damping values, expressed as percentage ratios to the critical damping value of the tube, were used in fluid-elastic stability analysis:

Swollen Tubes:

For 90% confidence estimates of fluid-elastic stability margins (FSM):
Top span, [b.c],
Bottom span, [b,c] including 0.02 from two-phase damping

For root cause analysis of Tube B66-130
Top span, [b,c] (lower bound of test data),
Bottom span, [b,c] including 0.02 from two-phase damping

In-service Tubes and Un-swollen Plugged Tubes:

Top span, [b,c],
Bottom span, [b,c]

Methodology, Model Inputs and Basis Specific to Turbulence-Induced Vibration

Based on recommendations from both ASME OM11 and ASME Sec III Appendix N1300, turbulence induced vibration due to axial flow was ignored and the joint acceptance method was used to estimate the turbulence-induced vibration amplitudes due to cross flow. The inputs are:

- The mode shape eigenvalues from the modal analysis, computed with the finite element model discussed previously under analytical models.
- Cross flow gap velocities, discussed previously under fluid-elastic instability analysis.
- Secondary fluid densities, discussed previously under fluid-elastic instability analysis.
- The fluctuating pressure power spectral density as represented by the empirical equation of Pettigrew and Gorman and recommended by the Sec III Appendix N non-mandatory code.
- The coherence range of the fluctuating pressure. This was obtained from measurement. Based on industry data a coherence range equal to 2.0 times the diameter of the OTSG tubes was used.
- Damping ratios. Since turbulence-induced vibration amplitudes are typically small, much smaller than those experienced at the threshold of fluid-elastic instability, the damping ratios used in turbulence-induced vibration may be smaller than those used in fluid-elastic stability analysis discussed above:

Swollen Tubes:

For 90% confidence estimates of fluid-elastic stability margins (FSM):
Top span, [b,c],
Bottom span, [b,c] including 0.02 from two-phase damping

For root cause analysis of Tube B66-130,
Top span [b,c],
Bottom span, [b,c] including 0.02 from two-phase damping

In-service Tubes and Un-swollen Plugged Tubes:

Top span, [b,c],
Bottom span, [b,c], including 0.02 from two-phase damping

Methodology, Model Inputs and Basis Specific to Vortex-Induced Vibration

As stated in ASME OM11 Appendix A, vortex-induced vibration in a tube bundle does not have the resonant, and usually detrimental consequence as in vortex-induced vibration of isolated tubes. The fluctuating pressure power spectra measured during the recent ten years showed broad peaks often attributed to vortex-induced excitation. Unlike in cross flow over isolated cylinders, these spectral peaks are not prominent peaks several orders of magnitudes higher than the off-resonance spectra, but are only 10-20 times higher than the spectra adjacent to this vortex excitation range. Following ASME Sec III Appendix N recommendation, vortex-induced vibration was calculated following the same method used in turbulence-induced vibration, with the following two modifications:

- In the frequency range within which vortex-shedding in the tube bundle can occur, the input fluctuating pressure power spectral density was adjusted higher to account for the higher forcing function associated with vortex-shedding.

- Since vortex-shedding is an organized, rather than random, event, the coherence range was set to an arbitrarily large number (such as 1000 tube diameters) to represent a coherent forcing function.

All the other inputs, including the damping ratios, are the same as those used in turbulence-induced vibration analysis.

Model Uncertainties

Generic Uncertainties:

The uncertainties common to calculating the FSM, turbulence and vortex-induced vibration come from

(1) uncertainty in the fluid-dynamic input;

(2) uncertainty in the damping ratio;

(1) Uncertainty in the fluid-dynamic input. The first uncertainty is addressed by using two different sets of input from two different sources, including the input from the "PORTHOS" computational fluid dynamics code and the older estimates that were actually extrapolated from a scale model test at the time the OTSGs were being designed. When all other input parameters are the same, the FSM values computed with these two different sets of fluid dynamic inputs are comparable, with the "PORTHOS" input giving results that are believed to be more accurate due to its more detailed modeling capability.

(2) Uncertainties in damping ratios. This is addressed by using two different values, one for design analysis and one for best-estimate analysis. The damping ratios used in FRA-ANP FIV analysis were derived from test data with tubes and support plates simulating those of the actual stream

FRA-ANP has traditionally used 3% normal structural damping associated with non-linearity of the tube to TSP clearance. Test results indicate that the non-linearity of the tube to TSP clearance provides about [b,c] damping. About [b,c] of this damping is lost as a result of a swelled tube. When the tube is internally pressurized, approximately [b,c] additional damping is created. This trend was also prevalent in the in-service tube and stabilized tube tests.

Uncertainties Specific to Fluid-elastic Stability Analysis: Uncertainties in the Connors' constant

The uncertainty in the damping ratio and the stability (Connors') constant is addressed together by using a conservative estimate of damping ratio of 3% for loosely supported multi-span tube together with a conservative value for the stability constant (3.3).

A test conducted at Babcock-Atlantique over 25 years ago showed that the stability constant for the OTSG tube bundle was about [b,c] while most of the industry data show stability constants over 4.0. An in-air test of the full size OTSG conducted 25 years ago showed that even with moderate vibration amplitudes well below the half tube-tube gap clearance, damping ratios mostly exceed 3%. Recent tests in the lab using a one span beam with real OTSG support showed a damping ratio close to 3% even for vibration amplitudes in the 0.01inch range. Therefore, FRA-ANP believes that the critical input parameters used in FIV analysis of OTSG tubes are conservative, and results in a conservative FSM. This supports using an FSM of 1.0 as the design requirement, if conservative inputs are used in the analysis.

Uncertainties in Turbulence Induced Vibration Analyses

In addition to uncertainties caused by uncertainties in the damping ratios, the results in turbulence induced vibration are governed by two additional input parameters that can only be determined approximately: the fluctuating pressure power spectral density and its coherence range. Except in the frequency range in which vortex-induced excitation

is present, Pettigrew and Gorman's empirical random pressure power spectral density are known to be conservative. In addition, the input coherence range, which is assumed to be two times the tube diameter, is also conservative since it is larger than the hydraulic diameter of the OTSG tube bundle. Based on measurement involving flow in an annular flow channel, FRA-ANP estimated that the coherence range of fluctuating pressure is close to one half of the hydraulic diameter.

Uncertainties in Vortex Induced Vibration Analyses

The results in vortex induced vibration analysis are governed by the pressure power spectral density as well as the damping ratio. In the frequency range where vortex-induced excitation is present, the value of the random pressure power spectral density input bounded all the data available in the open literature and is conservative. The uncertainty in the coherence range disappears in vortex-induced vibration analysis as the force is assumed to be fully coherent in this case.

9. Discuss the qualification of the FIV model and supporting empirical data, both for cross flows involving saturated water in the lower bundle region and super heated steam in the upper bundle region.

Response:

The Chalk River Nuclear Laboratory performed a stability test on a full-scale model that consisted of a (7 x 9)-tube array of the lower three spans of the B&W 177 Fuel Assembly OTSG. The actual span lengths, TSP thickness, and tube-to-TSP clearances were properly simulated in this test. Results of these tests show that the tube bundle was unstable at a cross flow gap velocity of [b,c] ft/s.

An analytical model of the Chalk River test tube was created to evaluate the FIV techniques and methodologies performed by FRA-ANP. The purpose of the model was to determine how accurately the analytical technique could predict the onset of instability, not to demonstrate conservative predictions. The analytical models predicted a best-estimate FSM of [b,c] under the flow conditions where the model was observed to be unstable. This result was obtained when using a Connors' constant of 2.4, an axial damping ratio of [b,c] and a perpendicular damping ratio of [b,c] for the test above. Therefore, the overall analytical model predicted the instability threshold to within approximately [b,c]%.

FRA-ANP has consistently used a Connors' constant of 3.3 for single-phase flows in top spans, and in the bottom span even though it is likely higher due to the two-phase flow in that region. An axial damping ratio of [b,c] and a perpendicular value of [b,c] are employed in the FIV analysis of OTSG tubes. The [b,c] axial damping is used to account for the frictional losses occurring between the tube and tube support plates as the tube slides vertically through the support plate. The contradiction in the constants employed in FRA-ANP FIV analysis and those determined from the Chalk River test can be in part eradicated through the relation of damping and the Connors' constant. The FSM of a tube is proportional to the following parameters:

$$\beta\sqrt{\xi} = [b,c]$$

where β is the Connors' constant, and
ξ is the perpendicular damping ratio

The combination of these two input parameters is believed to be realistic by industry experts in the field of FIV. It closely corresponds to the Connors' constant of 2.4 and damping of [b,c] (or 2.4[b,c] = [b,c]) assumed in the calculation to correlate with the Chalk River test results. When β=[b,c] and ξ=[b,c] inputs are used, the fluid-elastic stability margin predicted for the Chalk River test setup is [b,c] at the observed onset of instability, that is, with an accuracy of about [b,c]%.

Connors' constant is a function of tube array geometry only. It is not governed by the tube span lengths or the fluid media. Therefore the results are applicable to the top span even though in the top span, the tube bundle is subjected to superheated steam flow.

10. Describe nominal FIV response (e.g., stability ratios or some other figure of merit) under normal operating conditions at key locations in the bundle, including Regions 1, 2, and 3. Are these nominal FIV responses high enough to contribute to fatigue usage factors? What is the associated alternating stress and mean stress level?

Response:

The three regions of the OTSG referred to in this response are the same as those defined in the NRC statement of Question No. 7. The figures and tables referred to in this response are located at the end of this attachment.

Top-Span (Regions 1 and 2) Fluid-Elastic Stability Margin

As shown in Figure 1, under normal operating conditions, the fluid-elastic stability margins (FSM) – defined as the ratio of the critical velocity to the mode-shaped-weighted average span cross-flow pitch (or gap) velocity – are larger for tubes close to the center of the OTSG, and are dependent on the axial load of the tubes. However, the dependence is not very sensitive below the buckling load of the tube. The computed FSM between an axial load of 0 and 250 lb compression is not large as shown in Figure 1. For the same axial load, the stability margin generally increases for tubes closer to the center of the OTSG. As shown in Column 2, Rows 1 and 2 of Table 1, at the boundary away from the lane (Region 1), the stability margin of an in-service tube with zero axial load is 3.2. With an axial load of 250 lb compression, it is still equal to 2.9. The latter would decrease to 1.9 (Table 1, Column 2, Row 3) for the tubes located at the points of highest cross-flow (peripheral tubes on both sides of the lane, or Region 2 tubes). All the above results are based on a damping ratio of [b,c]. Based on both laboratory tests on tube samples and in-air tests of a full-scale OTSG, this is a representative and still conservative damping value for an in-service OTSG

tube vibrating with fairly large amplitudes indicative of instability. As part of the analysis performed in support of the TMI-1 severed tube root cause assessment, stability margins between 1.1 and 1.3 were calculated for a swollen tube at the periphery of the tube bundle (i.e., Region 1) under normal operating conditions (Column 2, Row 6 of Table 1). Thus under normal operating conditions, even the worst-located in-service

tube has a much higher margin of safety against top-span fluid-elastic instability than a Region 1 swollen tube.

Top-Span (Regions 1 and 2) Turbulence-Induced Stresses

As the OTSG heats up or cools down, the tubes may experience various degrees of axial load. Tensile axial loads tend to stiffen the tubes, making them less susceptible to flow-induced vibration. Compressive axial loads have the opposite effect. Only dynamic stresses which contribute to fatigue failure have to be evaluated.

For the tubing in the top span, the flow-induced stresses due to two different mechanisms: turbulence-induced and vortex-induced, were calculated. Figure 2 shows the computed maximum turbulence-induced stresses (those occur at the secondary face of the upper tubesheet), based on a [b,c]% damping ratio representative of small-amplitude vibration in a low-density, single-phase fluid such as superheated steam in the top span of the OTSG. In general, turbulence-induced stresses increase with the distance from the center of the OTSG. Under normal operating conditions, turbulence-induced stresses are very small (less than 1000 psi, rms), even for the two peripheral tubes by the lane (Region 2). The fatigue usage due to turbulence-induced stresses is negligible. If we exclude the effect of fluid-elastic interaction force, which increases rapidly as the tube approaches instability, turbulence-induced stress in a swollen tube is actually smaller than that of the corresponding in-service tube (Table 1, Column 4, Rows 2 and 7). This is the result of the tensile axial load in the swollen tube, which increases its modal frequency. Based on a separate finite element analysis in support of the root-cause analysis of tube B66-130, it was estimated that due to Poisson effect, the tensile axial load in a swollen tube was about 1000 lb. The turbulence forcing function decreases exponentially with increase of frequency. Based on test data, for small amplitude vibrations, the swollen tube also has a higher damping ratio than that of a non-swollen tube ([b,c]) due to its plastic material properties.

The root-cause analysis results show that when the cross flow velocity is low compared with the critical velocity, fluid-structure interaction force is negligible compared with turbulence induced and damping forces. The projected fatigue lives of both the in-service and swollen tubes are limited by turbulence-induced vibration and are well over 1000 years. As the cross flow velocity approaches the critical velocity (fluid-elastic stability threshold approaches 1.0), fluid-structure interaction force, which manifests itself as a negative damping, starts to play an increasingly important role. The vibration amplitude due to turbulence increases beyond what is predicted by linear, frequency domain analysis. It is this fluid-structure interaction force coupled with the normal force due to flow turbulence that caused premature fatigue failure of tube B66-130.

Top-Span (Regions 1 and 2) Vortex-Induced Stresses

Because the top spans are in a single-phase fluid with flow outwards, some tubes may be subjected to vortex-induced vibration at some of the modes. The results are shown in Table 1, Columns 5 and 6. For the in-service tube and swollen tube, vortex-induced stresses are below the endurance limit of Inconel 600 (16,000 psi 0-to-peak based on Curve B, ASME Boiler and Pressure Vessel Code, Section III Sub-section NB, Paragraph NB-3222.4, 1989).

Bottom Span (Region 3) Fluid-Elastic Stability Margin

Figure 3 shows the computed fluid-elastic stability margins (FSM) for the in-service tube with a damping ratio of [b,c]% ([b,c] basic plus 2% due to the two-phase mixture). Unlike the top span, the minimum FSM in the bottom span does not occur at the peripheral tubes. This is because as the feed water enters the tube bundle through the water ports, it is heated and changes into a two-phase water steam mixture with a much larger specific volume than sub-cooled water. The cross-flow pitch velocity increases as the mixture density decreases to satisfy the continuity equation. As the feed water enters further into the tube bundle, it starts its upward turn. In the OTSG bottom span, the maximum cross-flow velocity occurs, not at the periphery of the tube bundle, but at a point approximately 52 inches from the center of the OTSG. This is where the minimum FSM occurs. Tube B66-130 is not located at or near the point of minimum bottom-span FSM, it is almost 57 inches from the center of the OTSG.

As shown in Figure 3 and also Table 2 (Column 2, Rows 1 and 2), the minimum bottom span FSM for a normal in-service tube is 4.0. The minimum bottom span FSM of a swollen tube at the same location is 3.0. The minimum bottom span FSM of tube B66-130 is between 5.4 to 6.5. Thus, the worst-located swollen tube would have a stability margin in the bottom span higher than that of the top-span active mode of the worst-located in-service tube (Region 2).

Since in the bottom span, the flow is inwards through the water ports, the cross-flow velocity is governed by the location of the tubes relative to the water port openings. The presence of an un-tubed open lane has no effect on the cross-flow velocity as in the top span.

Bottom Span (Region 3) Turbulence-Induced Stresses

The static axial load stresses in the bottom span during heat up and cool down are the same as in the top span and have been discussed in the previous section regarding turbulence-induced stresses for the top span. The maximum turbulence-induced stress in the bottom span occurs at the secondary face of the lower tubesheet. As in the bottom span fluid-elastic instability analyses, the highest turbulence-induced stresses do not occur in the peripheral tubes, but in tubes approximately 52 inches from the center of the OTSG (Figure 4). Under normal operating conditions, turbulence-induced stresses in in-service tubes are very small, less than 1000 psi rms (Table 2, Column 4, Row 2). The fatigue life of the bottom span is expected to be over 1000 years.

Because of the tensile axial load that increases its natural frequency, a swollen tube actually has smaller turbulence-induced stress than the corresponding in-service tube. At the location of tube B66-130, turbulence-induced stress is even smaller than those located 52 inches from the center of the OTSG.

Comparison of the computed stresses (Tables 1 and 2, Column 4) for the top and bottom span shows that when the cross flow velocity is much lower than the critical velocity, turbulence-induced stress in the bottom span of the worst-located tube is higher than that in the top spans of the peripheral tubes. However, all are low enough to give fatigue lives more than 1000 years.

Bottom-Span (Region 3) Vortex-Induced Stresses

Because of the two-phase condition in the bottom span and because the flow is inwards into the tube bundle in the bottom span, vortex-induced vibration is not likely to occur in the bottom span. Vortex-induced vibration for the bottom span is therefore not considered.

11. Describe changes in FIV responses in these regions for plugged tubes. Discuss all revisions to boundary conditions, applied loadings, and other model inputs and basis for these revisions compared to nominal conditions.

Response:
See response to Question 12.

12. For plugged tubes, describe changes in FIV response in these regions for plugged tubes if tubes become swelled. Discuss all revisions to boundary conditions, applied loadings, and other model inputs and basis for these revisions.

Response:

The three regions of the OTSG referred to in this response are the same as those defined in the NRC statement of Question No. 7. The figures and tables referred to in this response are located at the end of this attachment.

The above two questions (questions 11 and 12) are best answered together as swollen, plugged tubes are special cases of plugged tubes. The interior volume of a plugged tube is normally filled with air instead of primary water. This lowers its temperature and decreases its axial compressive load, which in turn increases its margin against fluid-elastic instability and reduced its turbulence-induced stress. To allow for the possibility that a plugged tube may be leaking and filled with secondary side fluid, FRA-ANP traditionally carries out FIV analysis of plugged tube assuming its interior volume is filled with secondary side fluid. This leads to more conservative estimates of both fluid-elastic stability margins and turbulence-induced vibration.

The swelling has five effects on the plugged tube. These apply to all the three regions:

(1) As the tube expands it fills up the gap clearance between the tube and the support plates. The tube becomes laterally restrained (clamped, instead of simply-supported, at the support plates). The separate spans are isolated from one another. Unable to dissipate energy to the adjacent spans, the top and bottom spans, which are subject to most of the cross-flow loads, will be more prone to flow-induced vibration.

(2) As the clearance between the tube and the support plate is reduced to zero, there will be no relative motion, and no interaction between the tube and the support plates. This will eliminate light contact interaction between these two components. However, light contact interaction or "typical operational wear" is the principal source of energy dissipation in vibrating heat exchanger tubes. Without wear the only damping of the tube will be from material and viscous damping. Both are much smaller than damping due to wear between the tube and the support plates.

(3) As the tube swells beyond the elastic limit of the Inconel 600 tubing material, plasticity increases the material damping from that of elastic Inconel 600.

(4) As the tube swells, the Poisson effect tends to shorten its length. Since the OTSG tubes are clamped at the top and bottom tubesheets, the Poisson effect induces a tensile load, estimated to be approximately 1000 lbs maximum in the tube. This tends to stiffen the tube and increases its modal frequencies.

(5) Finally, and to a much smaller extent than the above four factors, swelling also has an effect on the mode shape and thus the modal participation of the forces. Sometimes this can shift the least stable mode from one to the other.

These five effects can potentially counter-act one another. The overall effect on flow-induced vibration can be better or worse depending on the FIV mechanism.

Fluid-elastic Instability:

Fluid-elastic stability margins are linearly proportional to the modal stiffness. In the specific case of tube B66-130, the increase in the tube stiffness due to the Poisson effect was apparently not sufficient to overcome the span-isolation effect and the net loss of damping in the top-span active mode. The margin against fluid-elastic instability decreased significantly.

Turbulence-Induced Vibration:

For the same forcing function, turbulence-induced stresses are inversely proportional to the modal stiffness. In addition, the turbulence forcing function spectrum decreases exponentially with increase of frequency. These two effects together are enough to counter-act the span isolation effect due to tube swelling. In addition, since turbulence-induced vibration typically involves small amplitudes, tube-support plate interaction does not play a prominent role as in fluid-elastic instability. Therefore, turbulence-induced

stresses in swollen tubes may be smaller than those in the corresponding in-service tubes.

Plugged Tube Top-Span (Regions 1 and 2) Fluid-Elastic Stability Margin

In this analysis, it was assumed that the interior volumes of plugged tubes are filled with secondary fluid, with fluid densities corresponding to the shell side fluid densities at the same elevations. Since fluid-elastic stability margins are governed by modal stiffness and damping, the computed results will remain approximately the same if the interior of the tube is assumed to be filled with air. Based on analyses performed to support earlier tasks, it was assumed that there is negligible axial load in a plugged and un-swollen tube at normal operating conditions. Fluid-elastic stability margins for the top-span active modes of plugged tubes are presented in Figure 1 and also in Table 1, where the curve over-laps with that of an in-service tube without axial load. In general, un-swollen plugged tubes have smaller compressive axial loads than the corresponding in-service tube and have therefore slightly higher margins against fluid-elastic instability than the corresponding in-service tubes.

Plugged Tube Top-Span (Regions 1 and 2) Turbulence-Induced Stresses

Again the interior of the plugged tube is assumed to contain secondary-side fluid. If the tube contains air, its natural frequencies will be higher, resulting in smaller responses to turbulence. Thus, this assumption is conservative. As in the fluid-elastic instability analyses, turbulence-induced responses of a plugged tube are about the same as those of a similarly located in-service tube with zero axial load (Table 1, Column 4, Rows 1 and 4). Because a swollen tube has a tensile load that significantly increases its top-span active modal frequency, a swollen tube actually has lower stress than the corresponding plugged but un-swollen tube.

Plugged Tube Top-Span (Regions 1 and 2) Vortex-Induced Stresses

Because the top spans are in a single-phase fluid with flow outwards, some tubes may be subjected to vortex-induced vibration at some of the modes. The results are shown in Table 1, Columns 5 and 6. For non-degraded plugged tubes, either swollen or un-swollen, vortex-induced stresses are below the endurance limit of Inconel 600 (16,000 psi 0-to-peak).

Plugged Tube Bottom Span (Region 3) Fluid-Elastic Stability Margin

Fluid-elastic stability margins of bottom-span active modes of plugged tubes are plotted in Figure 3 as a function of distance from the center of the OTSG and are also given in Table 2. Plugged tubes generally have smaller margins against fluid-elastic instability compared with those of in-service tubes; but have higher margins compared with those of plugged and swollen tubes. This is because the assumption that plugged tubes are filled with secondary side fluid bias the non-structural mass of the tube towards the bottom span, resulting in a larger participation from the bottom-span active modes compared with that of a in-service tube. As in in-service tubes, the smallest margin

against fluid-elastic instability occurs at a distance about 52 inches from the center of the OTSG, where the cross-flow velocity is the highest.

The bottom span active modes of in-service, plugged and plugged and swollen tubes are all well above the instability threshold, with FSMs>3.0.

Plugged Tube Bottom Span (Region 3) Turbulence-Induced Stresses

Turbulence-induced stresses in the bottom span of in-service, plugged and plugged and swollen tubes are plotted, as a function of distance from the center of the OTSG, in Figure 4 and the maximum values are also given in Table 2. Much of the discussions on turbulence-induced stresses in the top span also apply to the bottom span. In particular, because the tensile load in swollen tubes increases the modal frequencies, turbulence-induced stresses in swollen tubes are lower than those in non-swollen tubes. Indeed, as shown in Row 4, Table 2, turbulence-induced stresses in swollen tubes are lower than those in the in-service tubes. This is due mainly to the higher modal frequencies of the swollen tubes.

Plugged Tube Bottom-Span (Region 3) Vortex-Induced Stresses

Vortex-induced vibrations are considered unlikely in the bottom spans of the OTSG because in the bottom span the secondary side mixture is two-phase. No vortex-shedding has ever been observed in two-phase flows.

13. Assess FIV response of plugged, swelled tube which has undergone axial failure or fish mouth in each of the regions. Discuss all revisions to boundary conditions, applied loadings, and other model inputs and basis for these revisions. Discuss the potential for the tips of such axial failures to propagate under continued FIV to circumferential failure.

Response:

When the internal pressure in the swollen tube is large enough to induce a hoop stress that is larger than the ultimate strength of Inconel 600, the tube will fail with the formation of an axial through-wall flaw sometimes referred to as a "fish-mouth crack." The internal pressure will be released. However, since there is an axial load on a swollen tube as a result of the Poisson effect, the tensile stress in the swollen, failed tube will remain. Initially the length of this axial flaw is still small compared with the span length of the tube while the azimuthal opening of the fish mouth flaw is unlikely to exceed 90 degrees because of the limited energy stored in the water volume inside the plugged tube. Thus, the fluid-elastic stability margins, turbulence and vortex-induced stresses are all representative of those of plugged and swollen tubes with 90-degree, 100% circumferential flaws computed with a stress concentration factor of 1.5. In this analysis it was found that the margins against fluid-elastic instability were not significantly affected by through-wall flaws up to 90-degrees circumferentially but with short (compared with the span length) axial lengths. The fatigue life of such flawed tubes will be limited by vortex-induced vibration to about 44 years.

Flow-induced vibration introduces bending stress that act in the axial direction. Thus, it will not contribute to rapid axial propagation of the fish-mouth tips that would require alternating stresses in the hoop direction. However, because of the Poisson effect, there will be some small amount of flow-induced alternating stresses in the hoop direction. Because of the high stress concentration factor associated with the tip of a fish mouth type crack, these stresses might contribute to slow propagation of the fish mouth crack, but only in the axial direction. Based on analysis, which considered a large axial and circumferential opening, through-wall axial flaws as long as 2.0 inches will not significantly affect the system stiffness and therefore the fluid-elastic stability margins.

14. Given a probability of detection of 50/50, how shallow a wear indication (through wall) would the bobbin probe inspection be expected to find?

Response:

FRA-ANP recently completed an OTSG-specific evaluation of the ability of a 0.510" bobbin coil probe to detect tube-to-tube support plate wear. The sample set used for the evaluation consisted of eleven OTSG pulled tubes and twenty OTSG machined samples obtained from the EPRI NDE Laboratory. The machined samples that were used in the evaluation were only those that were representative of OTSG TSP wear. All indications $\geq$ 16% through wall were detected. The probability of detection (POD) at 90% lower confidence level for this examination technique was measured at > 0.88 for flaws $\geq$ 16% through wall. All TMI Unit 1 primary, secondary, resolution, and independent analysts were required to demonstrate a POD $\geq$ 0.8 for flaws during site specific tests. The tube-to-tube wear indications identified in the tubes adjacent to B66-130 are tapered and similar to tube-to-tube support plate wear.

15. During the November 9, 2001 meeting, a slide was provided to the staff titled "Severed Tube Wear on Adjacent Tubes." (This slide has been attached as an addendum to Enclosure 2 to this meeting summary.) The slide indicates that an "actual wear rate of 62 mils/EFPY [effective full power year]" was utilized in your associated analysis. Provide a discussion of the origin of this wear rate and any uncertainties associated with the use of this wear rate.

Response:

The estimated wear rate of 62 mils per EFPY was determined by extrapolating existing data from wear tests on tubes in tube support plates. The initial assessment, which resulted in the 62 mils per EFPY, was based on testing done with Alloy 600 tubes in carbon steel support plates, and assumed that the wear coefficient of Alloy 600 on Alloy 600 would be similar. Subsequent to the 11/9/01 meeting, test data became available for Alloy 600 on Alloy 600, which indicated that the wear coefficient would be approximately 3.6 times higher than was used in the original evaluation. This resulted in a revised wear rate of 224 mils per EFPY. This number was used in the final risk evaluation.

The general approach taken was to adjust the wear rate for Alloy 600 tubes on carbon steel support plates by the following factors:

(1) The increased sliding velocity afforded by the larger gap between the impacting surfaces (tube to tube gap vs. tube to TSP gap)
(2) The higher wear coefficient due to the different materials
(3) An impact factor of 2.

The approach is explained in more detail in the following paragraphs.

Utilizing the velocity and density typical for a peripheral tube in the upper span, a bulk flow (drag) load against the severed tube, B66-130, of about 0.15 lb/inch was calculated. This results in a total load of about 7 lbs over the span. From a finite element model of the severed tube, the cantilevered span of B66-130 would be able to move about 2 inches (at the UTSF) under such a load. Therefore, even with considerable room for error, the adjacent tubes predominantly support the severed remnant and its stiffness has a negligible effect on the load. (The model predicted what had happened in the generator; the severed tube would impact the adjacent downstream tubes.)

From this, it was surmised that the loading (due to bulk flow) on the adjacent tubes is similar in magnitude to that seen in the tube-to-TSP interfaces during normal operation. The total wear, however, depends not only on the average normal force, but on the product of the normal force and the 'sliding distance' by which two surfaces move relative to one another over time.

Postulating that the cantilevered span is constrained only to move between adjacent tubes, for direct hits on adjacent tubes this allows an excursion of 0.25 inches (radial) from its original position, somewhat higher for hits between tubes. Assuming that the frequency content of the vibratory response will remain largely unchanged, the vibratory velocity of the remnant end, and therefore the wear rate, is proportional to its overall displacement. The vibration amplitude is limited to approximately 0.25 inches overall amplitude (radial). A typical clearance value for a tube within a TSP can be approximated at 0.005 inches.

From empirical data on tube wear in OTSGs, TSP wear rates have been estimated at [b,c]. The wear rates for alloy 600 on alloy 600 (tube-to-tube contact) have been shown to be approximately 3.6 times higher than those seen where alloy 600 wears against carbon steel (i.e., tube-to-TSP wear). Therefore, a typical tube to tube wear rate might be expected to be

3.6 *0.25 in/0.005 in.* [b,c] =[b,c] mils/EFPY.

Where

3.6	is the factor of increase in wear rate from Alloy 600 on carbon steel to Alloy 600 on Alloy 600 (based on testing)
0.25	is the tube-to-tube clearance, in.
0.005	is the tube-to-TSP clearance, in.
[b,c]	is the observed wear rate for Alloy 600 tubes on carbon steel support plates for top span flow conditions in OTSGs

A dynamic amplification factor of two is typically used to account for impact effects. Since B66-130 was obviously impacting B65-130, the actual wear rate is estimated at [b,c], based on this evaluation.

The major source of uncertainty in the above evaluation is in the assumptions used to extrapolate the wear rate obtained from tube-TSP tests to apply to tube-to-tube impact. The assumption that the normal force is similar is reasonable because it is due primarily to flow load, which is essentially the same in both the reference test and the TMI steam generator. The adjustment made to the sliding velocity (adjusting by the ratio of clearance between the impacting bodies), however, is more uncertain. The velocity could be significantly different from what was estimated, depending on a number of factors. For this reason, it is believed that the above estimate is accurate only within an order of magnitude.

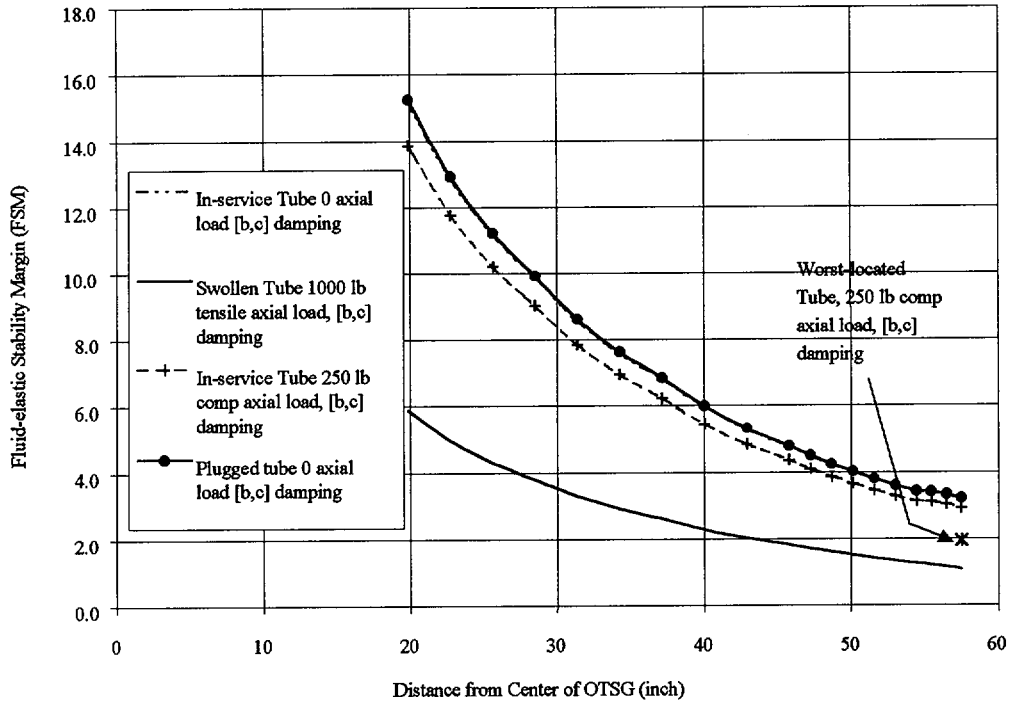

Figure 1: Top-Span Fluid-Elastic Stability Margins of In-service, Plugged and Swollen Tubes

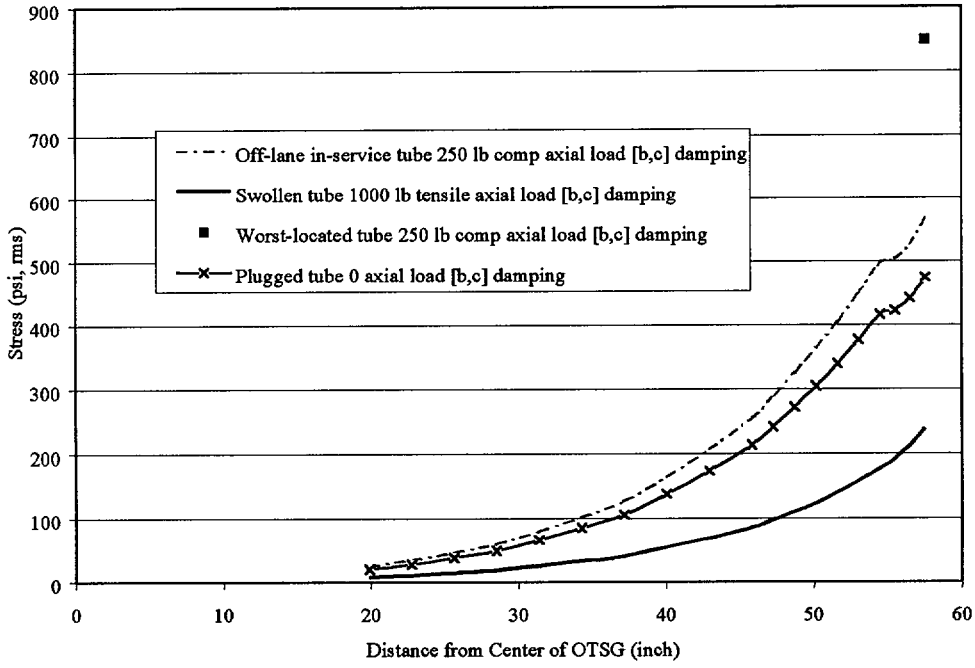

Figure 2: Top-Span Maximum Turbulence-Induced Stresses

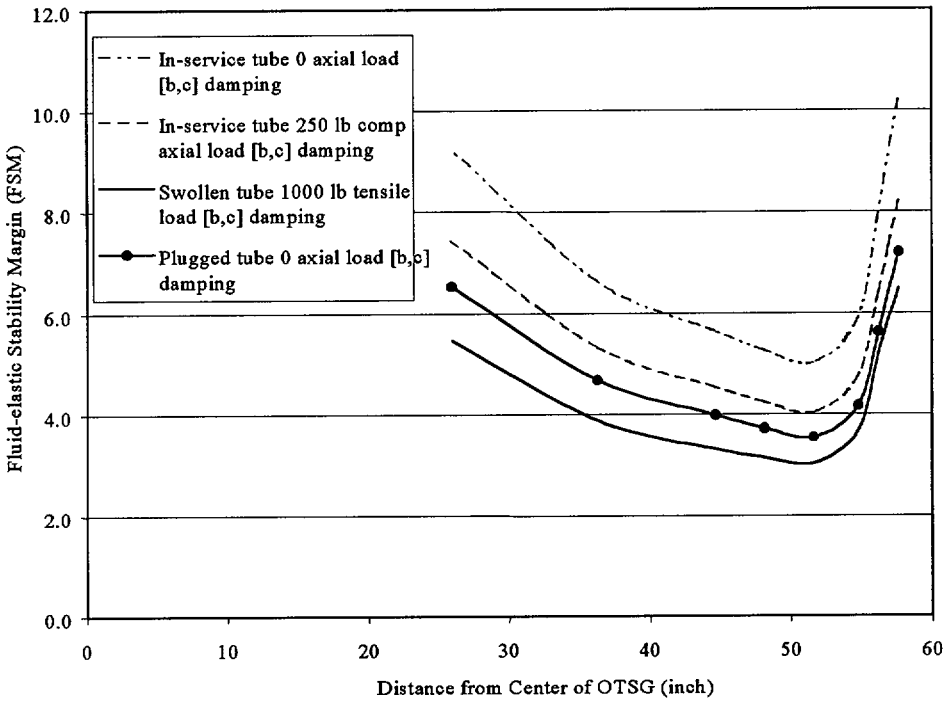

Figure 3: Bottom-Span Fluid-Elastic Stability Margins of In-service, Plugged and Swollen Tubes

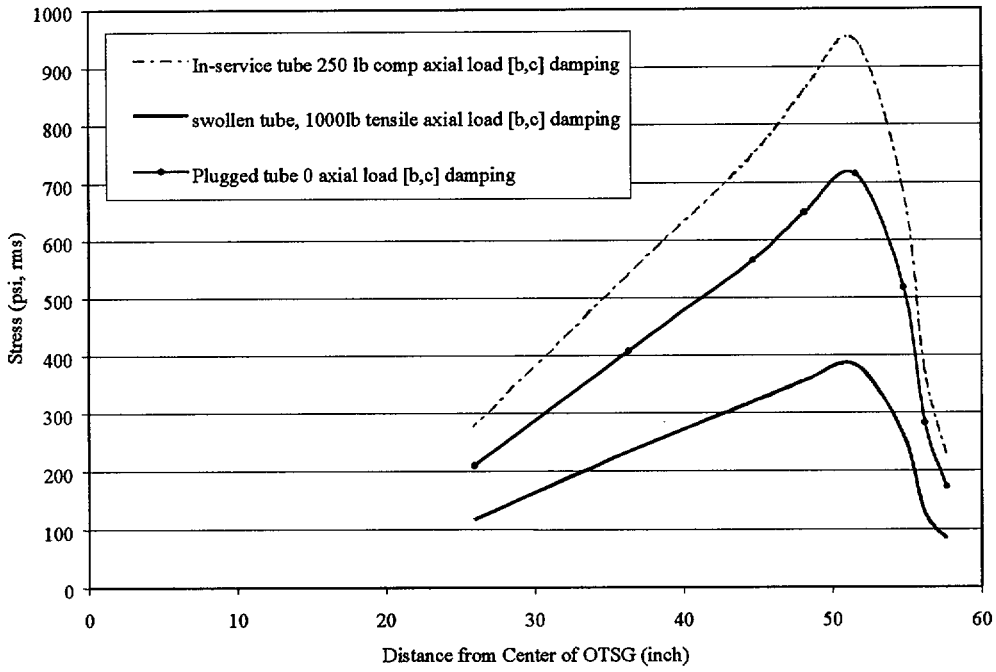

Figure 4: Bottom-Span Turbulence-Induced Stresses

Table 1: Summary of Results for Top Span[3]

Description	FSM	Turbulence-Induced Vibration [1]		Vortex-Induced Vibration[2]		Fatigue Life (years)
		Amplitude (inch, rms)	Stress (psi, rms)	Amplitude (inch, 0-p)	Stress (psi, 0-p)	
1	2	3	4	5	6	7
1. Worst non-lane In-service Tube, 0 axial load	3.2 (ζ=[b,c])	0.0055 (ζ=[b,c])	533	Not computed	Not computed	>1000
2. Worst non-lane In-service Tube, -250 lb axial load	2.9 (ζ=[b,c])	0.0063 (ζ=[b,c])	566	0.031	2823	>1000
3. Worst Located In-service Tube -250 lb axial load	1.9 (ζ=[b,c])	0.0142 (ζ=[b,c])	1274	0.070	6352	>1000
4. Worst non-lane Plugged Tube, 0 axial load	3.2 (ζ=[b,c])	0.0048 (ζ=[b,c])	475	0.030	6008	>1000
5. Worst Located Plugged Tube , 0 axial load	2.1 (ζ=[b,c])	0.0108 (ζ=[b,c])	1069	0.0675	13518	>1000
6. Swollen Tube, +1000 lb axial load	1.3 (ζ=[b,c]) 1.1 (ζ=[b,c])	0.0016 (ζ=[b,c])	239.4	0.017	3443	> 1000

(1) For Inconel 600, 3,300 psi rms can be considered the endurance limit for turbulence-induced stress.
(2) The endurance limit for Inconel 600 is approximately 16,000 psi 0-to-peak.
(3) The damping ratio, ζ , is given in the parentheses. ζ is the same for vortex and turbulence-induced vibration but is higher for large amplitude vibrations such as those experienced by an unstable tube.

Table 2: Summary of Results for Bottom Span
Note: B66-130 is not the worst case location and is calculated separately

Description	Worst-Located Tube				At B66-130			
		Turbulence-Induced Vibration				Turbulence-Induced Vibration		
	FSM	Amplitude (inch,rms)	Stress (psi, rms)	Fatigue Life (years)	FSM	Amplitude (inch,rms)	Stress (psi,rms)	Fatigue Life (years)
1	2	3	4	5	6	7	8	9
1. In-service Tube, 0 axial load	5.0 (ζ=[b,c])	Not Relevant	653 (ζ=[b,c])	>1000	10.2 (ζ=[b,c])	0.0016 (ζ=[b,c])	159 (ζ=[b,c])	>1000
2. In-service Tube, -250 lb axial load	4.0 (ζ=[b,c])	Not Relevant	946 (ζ=[b,c])	>1000	8.2 (ζ=[b,c])	0.0024 (ζ=[b,c])	229 (ζ=[b,c])	>1000
3. Plugged Tube, 0 axial load	3.6 (ζ=[b,c])	Not Relevant	715 (ζ=[b,c])	>1000	7.2 (ζ=[b,c])	0.0017 (ζ=[b,c])	300 (ζ=[b,c])	>1000
4. Swollen Tube, +1000 lb axial load	3.0 (ζ=[b,c])	0.0024 (ζ=[b,c])	383 (ζ=[b,c])	>1000	6.5 (ζ=[b,c])	0.00051 (ζ=[b,c])	83 (ζ=[b,c])	>1000

5928-01-20338
Attachment 3

"Adaptation of PORTHOS to the Once-Through Steam Generator"

R. W. Moore
Framatome Technologies, Inc.
Lynchburg, VA

ADAPTATION OF PORTHOS TO THE ONCE-THROUGH STEAM GENERATOR

R.W. MOORE
Framatome Technologies, Inc.
Lynchburg, VA

ABSTRACT

The PORTHOS Mod-01 computer code, developed by the Electric Power Research Institute, is a three-dimensional, transient thermal-hydraulic analysis tool for simulating two-phase flow in recirculating-type steam generators. Under the sponsorship of the Babcock & Wilcox (B&W) Owners Group, the PORTHOS code was modified for use in analyzing the Once-Through Steam Generator (OTSG). The goal has been to develop a tool to assess the effects of plugging tubes on the distributions of moisture and fluid velocities within the tube bundle under steady-state operating conditions in the OTSG.

The Mod-01 version of PORTHOS was modified to account for differences between the recirculating and once-through generators, particularly differences in the geometry and the operating heat-transfer regimes. Coding changes include (1) new routines for initializing the solution field, (2) revised flow boundary conditions to reflect the OTSG geometry, and (3) additions to heat transfer routines to model the film-boiling and steam superheat processes. The modified coding allows the user to optionally include the OTSG steam annulus as part of the solution domain and the bleed port as a boundary condition.

Pre- and post-processors were developed to automatically generate geometry input to the code and produce data output files to facilitate visualizing the flow-field solution with use of PATRAN.

Favorable results have been obtained in comparing the predictions of the OTSG-modified PORTHOS code with test data. PORTHOS results and test data agree well for both model boiler and full-size steam generator temperature profiles within the OTSG tube bundle. Good agreement has also been obtained for the predicted velocity distributions at the exit of the tube bundle in comparison with data from scale model tests.

NOMENCLATURE

c_{ps}	specific heat of vapor
g	acceleration of gravity
h_{FW}	enthalpy of feedwater
h_f	enthalpy of saturated liquid
h_{FB}	film-boiling heat-transfer coefficient
h_{fg}	latent heat of vaporization
h_s	enthalpy of steam
k_g	thermal conductivity of saturated steam
W_s	steam mass flow rate through steam generator bleed port
W_{FW}	feedwater mass flow rate through steam generator inlet spray nozzles
ρ_f	density of saturated liquid
ρ_g	density of saturated steam
μ_g	viscosity of saturated steam
ΔT_{sat}	temperature difference, wall to saturated fluid
σ	surface tension of liquid

INTRODUCTION

Local thermal-hydraulic conditions in nuclear plant steam generators may influence certain types of tube damage, such as denting, corrosion, and erosion. Also, the fluid velocity and density distributions in steam generators are of interest in evaluating margins to flow-induced vibration and the potential for wear, fretting, and high-cycle fatigue of the tubes.

During the late 1970s, efforts to develop a three-dimensional thermal-hydraulics model for simulation of the B&W Once-Through Steam Generator (OTSG) led to the development of the THEDA computer code (Ref. 1), supported by extensive model testing including both isothermal air tests at low temperatures and full-pressure model boilers. The fluid dynamic equations used in THEDA are based on the assumptions of homogeneous flow and thermal equilibrium between phases. Consequently, the usefulness of THEDA as a modeling tool for thermal-hydraulic analysis of the OTSG is limited, particularly in terms of the ability to model the phenomena associated with the carry-up of moisture droplets in the film-boiling and superheat heat-transfer regions of the generators.

The PORTHOS Mod-01 computer program (Ref. 2), hereinafter referred to as PORTHOS/RSG, is a three-dimensional, finite-difference, thermal-hydraulic analyzer that simulates transient two-phase flow in recirculating steam generators (RSGs). PORTHOS/RSG employs a six-equation mathematical model for the two-phase flow field. Equations are expressed in terms of surface and volume porosities, which allow complex geometries to be modeled. The capability of the model to simulate thermal non-equilibrium between phases is important for accurately predicting conditions arising in the OTSG, particularly the film-boiling heat transfer and dispersed-droplet flow processes.

Although PORTHOS/RSG is configured specifically for simulating RSGs, the code is constructed in a modular form that facilitates making modifications for simulating other geometric configurations. This article describes changes made to the computer code for analyzing the B&W OTSG and presents results of comparisons with previously existing test data. Hereinafter, the modified version of PORTHOS is referred to as PORTHOS/OTSG.

Modeling the OTSG Shell-Side Geometry

The PORTHOS/OTSG model includes the tube bundle and steam annulus regions. The detailed geometry of the tube bundle, including the TSPs, is specified by generating the appropriate volume porosities and surface permeabilities for cells of the computational mesh using a pre-processor. For modeling the OTSG, PORTHOS includes the steam annulus in the solution domain since the annulus geometry strongly influences the fluid velocity distribution at the outlet of the tube bundle as well as over the top span between the uppermost TSP and the upper tubesheet. The fluid boundary condition at the steam outlet nozzles of the steam annulus is specified as a constant pressure.

The finite-element mesh of the model excludes the feedwater downcomer region and the associated process of direct contact heating of the feedwater. The preheating of subcooled feedwater via steam condensation is simulated separately to circumvent potential numerical instabilities. This simulation entails calculating the bleed port flow required to heat the feedwater to saturation under steady state conditions. Calculation of the bleed port steam flow rate is based on an energy-conservation equation with the downcomer as the control volume; the thermal energy convected into the downcomer (feedwater and aspirated steam) equals the energy flowing out of the downcomer, or

$$W_S h_S + W_{FW} h_{FW} = (W_S + W_{FW})\, h_f \,. \qquad (1)$$

The flow rates through the bleed port and the feedwater inlet spray nozzles are summed to determine the flow rate entering the tube bundle at the feedwater inlet port. Flow-related boundary conditions are imposed on the thermal-hydraulic solution domain at the tube bundle inlet and bleed ports by assigning fluid enthalpies and/or velocities at appropriate faces of cells in the finite-difference mesh.

PORTHOS/RSG provides a transient solution option; however, the steady-state energy equation used to calculate the bleed port and bundle inlet flow rates in this case limits the use of PORTHOS/OTSG to steady-state predictions. Since the 3-D flow field parameters are initialized by first generating a one-dimensional approximation to the solution, the thermodynamic properties of the steam drawn through the aspirator port will change during the iterative process of arriving at the final, converged solution. The changes necessitate updating the fluid boundary conditions at the bleed port and bundle inlet at each iterative cycle.

OTSG Shell-Side Heat Transfer

Differences in operating heat-transfer regimes of the recirculating and once-through steam generators necessitates changing the heat-transfer modeling in PORTHOS. Normal steady-state operation of the U-tube recirculating steam generator involves bulk, and possibly subcooled, boiling regimes. However, the normal operating heat-transfer regimes in the OTSG include bulk boiling, film boiling, and forced convection of superheated steam.

In the OTSG, where the evaporating liquid film on the tube ceases to exist at the end of the nucleate boiling region, a small amount of liquid remains in the form of entrained droplets in the vapor. Concurrently, the vapor may be superheated. Any liquid droplets remaining at the exit of the tube bundle are normally evaporated by mixing with superheated steam prior to the fluid leaving the steam generator at the steam outlet nozzles.

The approach used to calculate shell-side heat transfer in the PORTHOS/OTSG model is outlined below. This approach is similar to that used in PORTHOS/RSG except for the addition of equations describing the film-boiling process. The film-boiling regime in the PORTHOS/OTSG model applies at values of void fraction ranging between 0.995 and 1.0.

Partitioning of heat flow

In the nucleate boiling regime, heat transfer from the tube wall to the fluid is partitioned to the liquid and vapor, based on wall contact surface area fractions for each phase. Wall contact surface-area fractions vary as functions of the value of void fraction, as described in the PORTHOS manual (Ref.2).

Heat transfer to vapor

Heat transfer to vapor is by forced convection in all regimes, i.e., nucleate boiling, film boiling, and superheat. The Dittus-Boelter forced-convection film coefficient is employed.

Heat transfer to liquid

Nucleate boiling

The film coefficient for heat transfer to liquid is calculated by summing forced-convection (Dittus-Boelter) and nucleate-boiling (Thom) coefficients.

Film boiling

Heat transfer to liquid is calculated using the modified Bromley film coefficient, h_{FB}, as follows (Ref. 3):

$$h_{FB} = 0.62\left[\frac{k_g^3 \rho_g (\rho_f - \rho_g)\, h'_{fg}\, g}{\lambda_c \mu_g\, \Delta T_{sat}}\right]^{0.25} \qquad (2)$$

where

$$h'_{fg} = h_{fg} + 0.5 c_{pg}\, \Delta T_{sat} \qquad (2a)$$

$$\lambda_c = 2\pi\left[\frac{\sigma}{g(\rho_f - \rho_g)}\right]^{0.5} . \qquad (2b)$$

PORTHOS/RSG MODEL DESCRIPTION

The PORTHOS computer code manual (Ref. 2) describes the mathematical model used for the two-phase secondary-side flow, including the basic equations for conservation of momentum and energy, and the finite-difference forms of these equations. It also describes the method of solution for the system of equations, which involves an iterative procedure. The equations for modeling interphase drag, mass transfer, and heat transfer in the code are given, including equations for the heat transfer from primary to secondary fluid. The PORTHOS/RSG heat-transfer model includes partitioning the heat flow from the tube surface to the secondary-side liquid and vapor phases. PORTHOS/RSG also models interphase heat transfer.

A typical RSG model includes the downcomer between the tube bundle wrapper and vessel shell, and the region inside the wrapper from the tubesheet to the entrance to the steam separators. PORTHOS does not treat the steam separators as part of the two-phase flow solution domain. The injection of feedwater can be modeled either at the elevation of the top of the downcomer or at a separate port, such as near the tubesheet. Economizer sections may be included in the model. A complete description of the geometry in the solution domain is generated using a pre-processor. This pre-processor describes the volume porosities, surface permeabilities, and dimensions of each computational cell of the finite-difference grid.

PORTHOS/OTSG MODELING

Modifications made to PORTHOS to model the OTSG deal primarily with changes in (1) the geometry describing the solution domain, and (2) heat-transfer regimes and correlations.

Description of the B&W OTSG

The B&W-designed OTSG (Figure 1) is a vertical, straight-tube, single pass, counterflow heat exchanger with shell-side boiling. The primary-side flow enters the upper head through a single inlet nozzle, passes downward through more than 15,000 tubes with an effective heat transfer length of 52 feet, and exits the lower head through two outlet nozzles. On the secondary side, subcooled feedwater is sprayed downward into the annulus formed by the shell and the tube bundle shroud where it is heated to saturation by condensing steam aspirated from the tube bundle. The combined flow, at saturated conditions, drops to the bottom of the downcomer and enters the tube bundle where steam is generated by nucleate boiling. As the secondary-side mixture rises and reaches a point slightly above the mid-bundle elevation, dryout occurs over most of the bundle cross section. The steam becomes superheated in the upper section of the bundle and any remaining moisture, in the form of droplets entrained in the flow, is evaporated. Steam flow exits the bundle radially through the gap extending around the entire bundle circumference between the secondary face of the upper tubesheet and the top of the shroud. The flow continues down the steam annulus, and exits the OTSG through two outlet nozzles to the main steam system piping.

The nominal OD of the tubes is 5/8-inches. Tubes are spaced on a triangular pitch, laterally supported by tube support plates (TSPs) at fifteen axial locations. The TSP broached-hole geometry provides radial support at three equally spaced points around the circumference of each tube. In the B&W design, one-half of the center row of tubes is omitted, forming an untubed lane extending from the center to the outer radius of the bundle. The geometry of the broached TSP openings in the untubed lane is identical to that of the tubed positions of the bundle.

At the center of the tube bundle is a small untubed region, in which the axial flow is largely blocked at the TSP locations. At the outer periphery of the tube bundle, a gap exists between the outermost tubes and the shroud; the width of this gap is about twice the bundle tube pitch. The axial flow paths through the peripheral gap region are either partially or totally blocked at the TSPs.

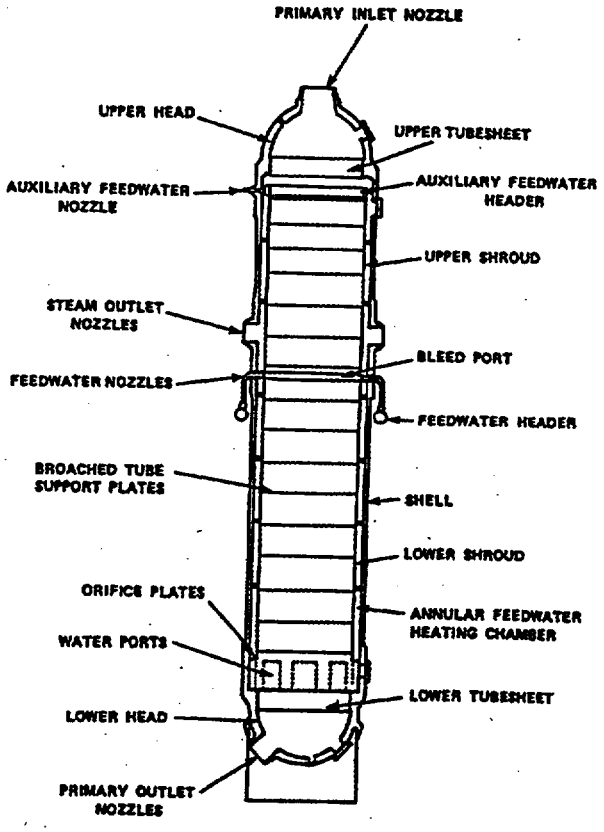

FIGURE 1 177 SERIES ONCE-THROUGH STEAM GENERATOR

COMPARISONS WITH TEST DATA

PORTHOS/OTSG models have been constructed for test boilers and full-sized steam generators to compare predictions with measured data. Available test data include (1) axial temperature and pressure distributions for a 19-tube model boiler, (2) steam generator shell-side fluid temperature measurements obtained during initial startup of Unit 1 at Duke Power Company's Oconee Nuclear Station, and (3) shell-side fluid velocity distributions at the tube-bundle exit of a one-half scale model test rig flowing air.

19-Tube Model Boiler Data

Figure 2 shows the predictions of PORTHOS for the axial temperature distributions in a 19-tube, full-length model boiler. The test conditions for Run 98 are representative of the power level and secondary-side flow rates at which the full-sized OTSG normally operates. Shown in the figure are the primary-side fluid, tube wall, and secondary-side fluid temperatures versus axial distance above the lower tubesheet. The predictions for secondary-side fluid is for steam; the liquid temperature is nearly constant over the entire length, at the saturation value.

Nucleate boiling extends about 25 feet above the lower tubesheet in this test (Run 98) as evidenced by the sudden change in the trend of tube temperature with axial distance. From this point to about the 40-foot elevation, measured fluid temperatures show considerable scatter; this is caused by liquid droplets wetting the thermocouples which are mounted on the tube wall and extend a short distance into the fluid stream. PORTHOS predictions for the axial distribution of void fraction, shown in Figure 3, are reasonably consistent with the fluid temperature data, indicating the presence of liquid droplets in the flow up to about the 35-foot elevation (where the calculated void fraction reaches a value of 1.0).

Figures 4 and 5 (Run 99) show information similar to Run 98, but for a higher-than-normal shell-side flow rate, producing a longer boiling length and lower exit superheat steam temperature. In this case, measured fluid temperatures and the calculated void fraction indicate the presence of liquid droplets in the flow up to about 48 feet. Results for both test conditions demonstrate the capability of PORTHOS to accurately model the flow process in the superheat region of the OTSG, where a significant degree of thermal non-equilibrium exists between the two phases.

The PORTHOS/OTSG predictions of tube-metal temperatures are for the wall mid-point. However, the sensor locations in the test rig are at the outside wall surface, thus explaining the differences between predicted and measured wall temperatures seen in the comparison plots.

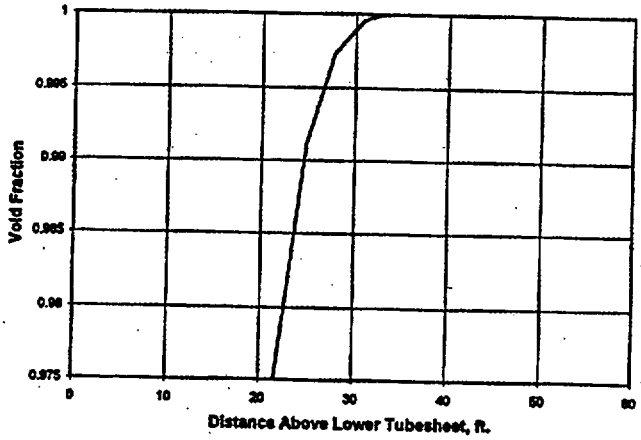

FIGURE 3. PORTHOS PREDICTION, AXIAL DISTRIBUTION OF VOID FRACTION (RUN NUMBER 98).

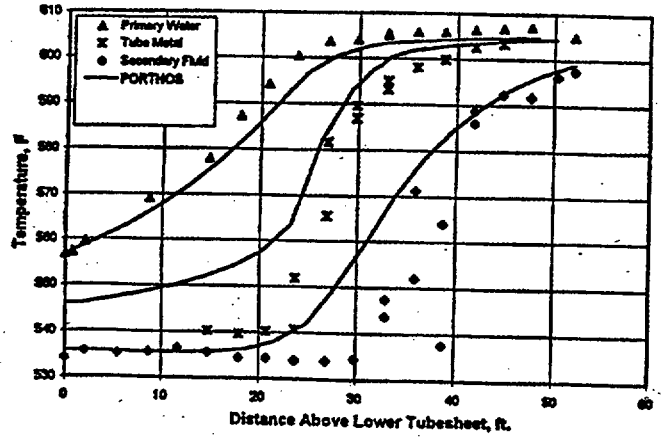

FIGURE 2. COMPARISON OF PORTHOS AND 19-TUBE MODEL BOILER DATA, AXIAL TEMPERATURE PROFILES (RUN NUMBER 98).

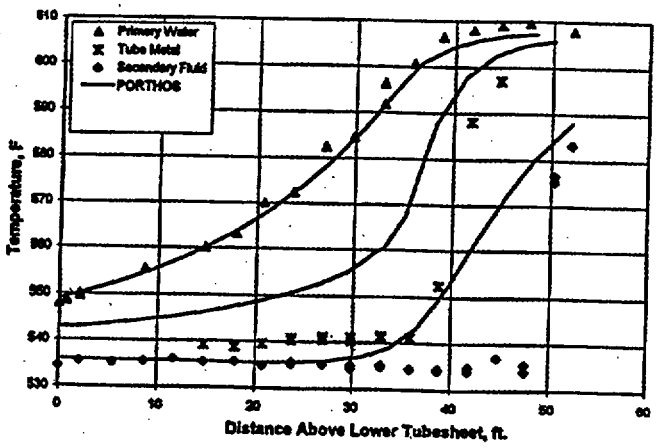

FIGURE 4. COMPARISON OF PORTHOS AND 19-TUBE MODEL BOILER DATA, AXIAL TEMPERATURE PROFILES (RUN NUMBER 99).

Figure 6 shows the PORTHOS predictions and test data for the axial pressure profile in the 19-tube boiler in Run 001A, with operating conditions similar to those of Run 98, above. Fluid pressure differences shown are relative to the boiler outlet pressure. An empirical constant input to PORTHOS/OTSG for the concentrated hydraulic resistance of the TSP produces a good match of the pressure profile of the test data for the full range of fluid quality along the axis of the boiler.

Oconee Nuclear Station Unit 1 Startup Data

Figure 7 shows radial temperature distributions at the tube-bundle outlet, comparing PORTHOS predictions and test measurements from the Oconee Unit 1 steam generator at an elevation approximately one foot above the uppermost TSP. Test data shown are for operation at 95 percent power. The decrease in steam temperatures toward the outer radius of the bundle is a result of lower temperature steam in the vicinity of the peripheral gap between the tube bundle and shroud. Temperatures are shown for locations along the bundle radius diametrically opposite the untubed lane.

Plant temperature measurements taken at radial locations along the untubed lane region, register fluid temperatures at saturation. PORTHOS results predict the presence of moisture in the untubed lane region at this elevation and operating condition, consistent with the temperature measurements.

One-Half Scale Model Air Flow Test Data

Figure 8 compares PORTHOS predictions and test measurements for the axial distribution of radial velocities over the top span at the outer bundle radius for a fully-tubed, wedge-shaped section of the steam-generator bundle. The peak

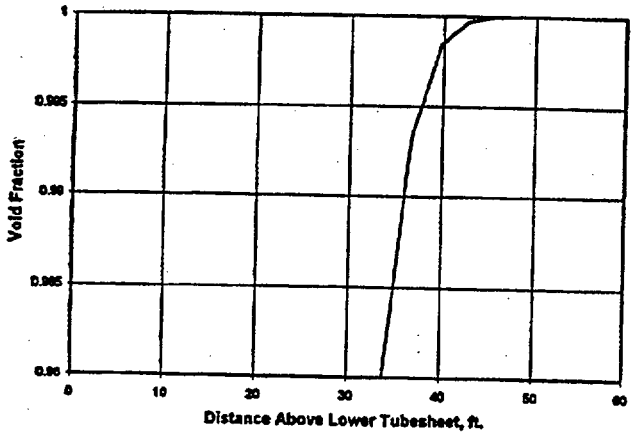

FIGURE 5. PORTHOS PREDICTION, AXIAL DISTRIBUTION OF VOID FRACTION (RUN NUMBER 99).

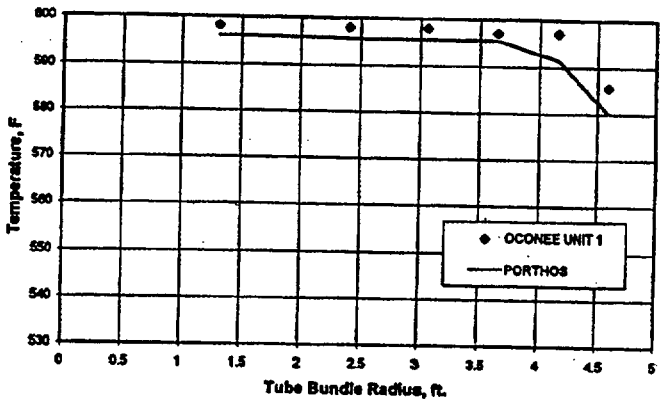

FIGURE 7. COMPARISON OF PORTHOS PREDICTIONS WITH PLANT MEASUREMENTS, RADIAL TEMPERATURES AT OTSG OUTLET

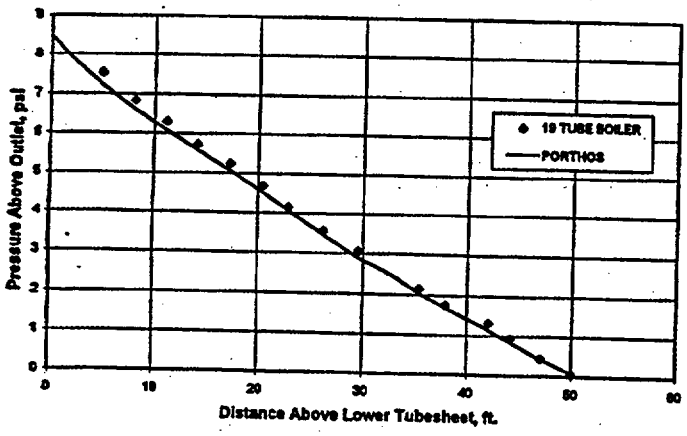

FIGURE 6. COMPARISON OF PORTHOS PREDICTION WITH 19-TUBE MODEL BOILER DATA, AXIAL PRESSURE PROFILE (RUN NUMBER 001A).

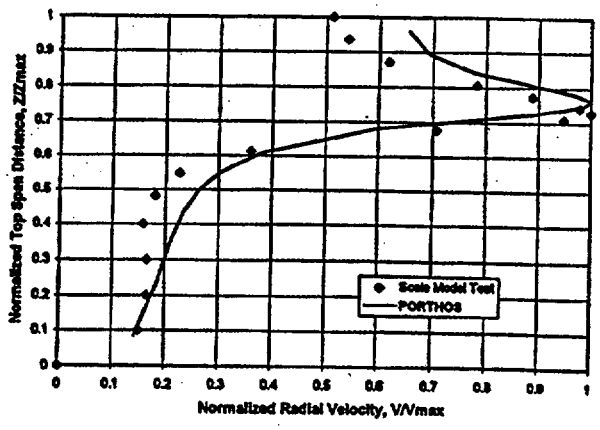

FIGURE 8. COMPARISON OF PORTHOS PREDICTIONS WITH SCALE MODEL TEST DATA, RADIAL VELOCITY PROFILE AT BUNDLE OUTLET.

velocities predicted by PORTHOS and the measured radial fluid velocities of the scale-model test rig both occur at an elevation slightly above the top of the shroud surrounding the tube bundle.

CONCLUSION

The PORTHOS computer code has been successfully adapted to the B&W OTSG geometry and fluid operating conditions. Good agreement exists between calculated results and test data for temperature, pressure, and velocity distributions of the steam generator shell-side flow field. Based on these results, PORTHOS/OTSG is a reasonably accurate analytical tool for predicting local fluid conditions in the OTSG, providing the analyst with the means to assess the effects of changes in plant operating conditions such as increases in power rating and in the number of plugged tubes.

REFERENCES

1. Fortino, R.T., et. al.,"THEDA-2: A Multidimensional Steam Generator Thermal-Hydraulic Model," EPRI NP-3031-CCM, December 1983.

2. Masiello, P.J., "A Computer Program for Three-Dimensional, Two-Fluid Model Thermal-Hydraulic Simulation of Steam Generators: PORTHOS Mod-01, Volume 1: Theory and Method of Solution," Project S411-1, EPRI NP-6891-CCML, July 1990.

3. Bjornard, T.A. and Griffith, P., "PWR Blowdown Heat Transfer," ASME Symposium on the Thermal and Hydraulic Aspects of Nuclear Safety, November 27-December 2, 1977, 1, pp. 17-39.